Fiducial Reference Measurements for Ground-Based DOAS Air-Quality Observations

ESA Contract No. 4000135355/21/I-DT-lr

Deliverable D1.2:

Algorithm Theorical Basis Document (ATBD)

Date: 14/10/2022

Version: 1b

Contributing authors:

F. Hendrick, M. Friedrich, M. Van Roozendael (IASB-BIRA)

A. Richter (IUP-UB)

U. Friess (IUP-HD)

A. Piters (KNMI)

T. Wagner (MPIC)

M. Navarro and M. Yela (INTA)

A. Bais and D. Karagkiozidis (AUTH)

Content

Acronyms and abbreviations

Acronyms and abbreviated terms that are specific for this document can be found below.

AFGL	Air Force Geophysics Laboratory
AK	Averaging Kernel
AMF	Air Mass Factor
ASCII	American Standard Code for Information Interchange
ATBD	Algorithm Theoretical Basis Document
CTM	Chemistry Transport Model
DISORT	Discrete-Ordinate Radiative Transfer model
DOAS	Differential Optical Absorption Spectroscopy
DOFS	Number of Degrees of Freedom for Signal
DSCD	Differential Slant Column Density
ECMWF	European Centre for Medium-Range Weather Forecasts
EDE	Extra-DSCD error
FRM_4DOAS	Fiducial Reference Measurements for Ground-Based DOAS Air-Quality Observations
FWHM	Full Width at Half Maximum
HWHM	Half Width at Half Maximum
LUT	Look-up table
MPIC	Max-Planck Institute for Chemistry
NDACC	Network for the Detection of Atmospheric Composition Change
OEM	Optimal Estimation Method
RTM	Radiative transfer model
SLIMCAT	Single Layer Isentropic Model of Chemistry And Transport
SCD	Absolute Slant Column Density
SZA	Solar zenith angle
VCD	Vertical Column Density
WF	Weighting Function

1 Introduction

The present document is the ATBD (Algorithm Theoretical Basis Document) for the new version of the stratospheric NO_2 profiling algorithm developed as part of the FRM_4DOAS-2.0 project. The purpose of the ATBD is to provide detailed mathematical and physical descriptions of the algorithm, along with a description of the main related random and systematic uncertainty sources. The present ATBD focusses only on the profiling part of the retrieval. The physical description of the DOAS method (including the spectral fit settings) used to retrieve the NO_2 slant columns densities that are ingested by the profiling algorithm can be found in https://frm4doas.aeronomie.be/ProjectDir/Deliverables/FRM4DOAS_D6_MAXDOAS_Algorithm_ATBD_v02_20180130.pdf. The document is structured as follows: the main principle of the stratospheric NO_2 profile retrieval from twilight zenith-sky DOAS observations is presented in Section 2. The consolidated FRM_4DOAS profiling algorithm and corresponding settings are described in Section 3. The assessed error budget is presented in Section 4. The vertical sensitivity and horizontal representativeness of the retrieved profiles are discussed in Sections 5 and 6, respectively. References used in this document are given in Section 7.

2 Stratospheric NO_2 profile retrieval

2.1 Main principle

The inversion of stratospheric NO_2 vertical profiles from twilight zenith-sky NO_2 DSCDs observation is based on the dependence of the mean scattering height with SZA: during twilight, as the SZA increases, the mean scattering height rises into the absorber layer (20 to 40 km for NO_2; see Figure 1), so each slant column measurement is mainly representative of the absorber concentration in a given altitude range. The observed slant column variation during twilight depends therefore on the vertical distribution of the trace gas and the latter can be retrieved by applying a linear OEM approach (see Preston et al., 1997; Hendrick et al., 2004) to the measurement vector *y* consisting in a set of measured twilight (sunrise or sunset) NO_2 DSCDs usually measured in the 75-94°SZA range.

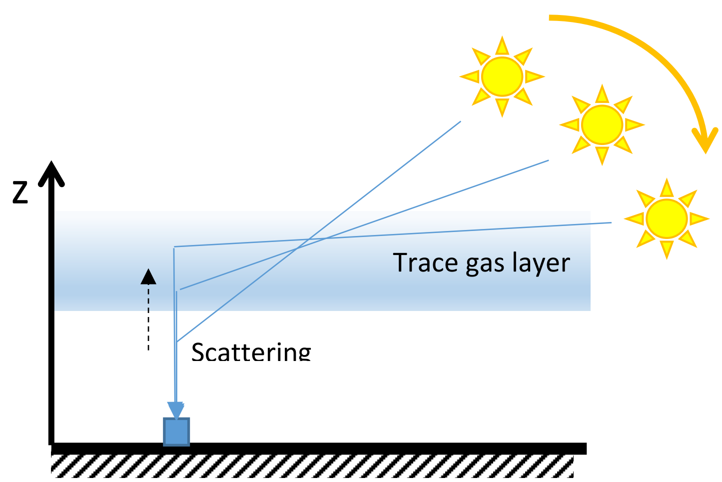

Figure 1: sketch of the twilight zenith-sky geometry used for the stratospheric NO_2 vertical profile retrieval.

In the case of NO_2, the simple geometric dependence on which the profiling approach is based, is complicated by the rapid variation of NO_2 concentrations with local SZA at twilight due to photochemistry (see Figure 2). In order to calculate appropriate WFs, it is therefore important to use a RTM that accounts for the 2D (altitude, SZA) photochemical variation of NO_2, at least for the incident beam (first order approximation). The 2D NO_2 concentration fields used as an input to the RTM are taken from stacked box photochemical model simulations initialized with 3D-CTM meteorological and chemical fields extracted at the location of the station (Hendrick et al., 2004).

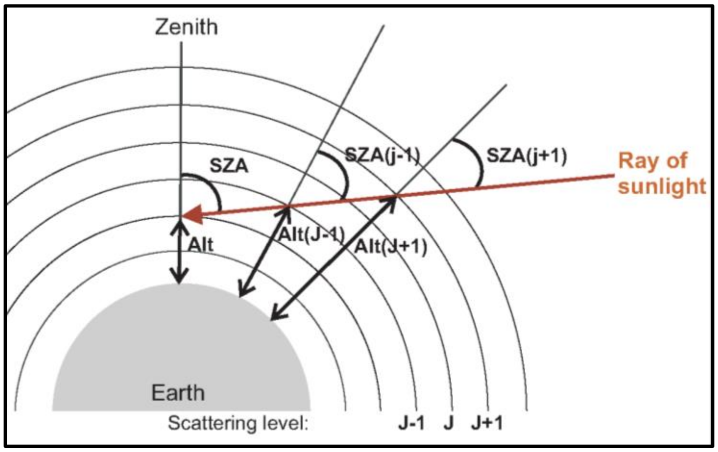

Figure 2: Variation of the local SZA along the path of a given ray. SZA(j)=local SZA of the ray in the jth scatter level.

2.2 The OEM approach

In the OEM formalism (Rodgers, 2000), a profile x is retrieved given an a priori profile x_a, the measurements y (DSCDs as a function of scan elevations for tropospheric NO_2 or HCHO profiles), their respective uncertainty covariance matrices (S_a and S_ε, respectively), and the matrix K of the WFs that indicate the sensitivity of the differential slant column abundances at each SZA to a change in the vertical profile:

$$x = x_a + S_a K^T (K S_a K^T + S_\varepsilon)^{-1} (y - K x_a) \text{ with } K = \frac{\partial y}{\partial x} \text{ and } K^T \text{ is the transpose of } K \qquad (1)$$

The weighting functions have been determined by consecutively perturbing each layer of the a priori profile and recalculating the set of measurements using a RTM as forward model. The OEM for linear case is considered for optically thin absorbers like NO_2 because measured DSCDs depend linearly on the concentrations in each profile layer. Therefore the WF matrix K is independent of the state (Heskes and Boersma, 2003) and a single inversion step is sufficient.

The a priori profile x_a and the S_a and S_ε covariance matrices are key parameters for the retrieval. Because the inversion problem is ill-posed (there are more elements in the state vector x than independently measured elements in the vector y and therefore no unique solution to Eq. 1), a priori constraints are necessary to reject unrealistic solutions that might be consistent with the measurements. In the case of stratospheric NO_2 profile retrieval, a priori profiles are usually taken from the output of a 3D-CTM model.

Since the residuals from the DOAS fitting are in most cases dominated by the random noise of the detector, the measurement covariance matrix S_ε is chosen diagonal with values corresponding to the statistical errors on the trace gas DOAS fit. The S_ε matrix being fixed, the a priori covariance matrix S_a can act like a tuning parameter (see e.g. Schofield et al., 2004). The variance value to be placed on the diagonal of the S_a matrix is empirically determined for each {trace gas, FRM_4DOAS station} pair based on dedicated sensitivity tests. The selected variance value should maximize the information content (DOFS; see Section 5 below) without leading to undesired oscillations in the retrieved profiles. S_a also contains extra-diagonal terms in order to account for correlations between trace gas concentrations at different altitude levels. These terms are usually added as Gaussian functions as follows (Barret et al., 2002):

$$S_{a\,ij} = \sqrt{S_{a\,ii} S_{a\,jj} e^{-\ln(2)\left(\frac{z_i - z_j}{\gamma}\right)^2}} \quad (2)$$

where z_i and z_j are the altitudes of i^{th} and j^{th} levels, respectively, and γ is the HWHM (half of the correlation length).

3 FRM4DOAS stratospheric NO_2 profiling algorithm

The OEM-based profiling algorithm developed at BIRA-IASB for the inversion of NO_2 vertical profiles from twilight zenith-sky NO_2 DSCDs (see Hendrick et al., 2004) has been implemented in the FRM4DOAS central processing system as part of the phase I of the FRM4DOAS project. The main theoretical principles on which this algorithm is based are given in the previous Section. Only the settings specific to the BIRA-IASB tool are described here.

The forward model consists of the stacked box photochemical model PSCBOX (Errera and Fonteyn, 2000) coupled to the RTM package UVSPEC/DISORT (Mayer and Kylling, 2005). As mentioned in Section 2, a photochemical model is required to reproduce the effect of the rapid variation of NO_2 concentrations at twilight and the RTM is used to calculate SCDs/WFs from the NO_2 concentrations predicted by the photochemical model.

The PSCBOX model includes 48 variable species, 141 gas-phase photochemical reactions as well as heterogeneous reactions on liquid sulfuric acid aerosols and on solid nitric acid trihydrate (NAT) and ice particles. It is initialised daily at 20 independent altitude levels (between ~10 and ~55 km of altitude) with 0h UT meteorological and chemical fields from the 3D CTM SLIMCAT (run 509; see Chipperfield, 2006). The chemical timestep is 6 minutes; no family and photochemical equilibrium assumptions are made. In the consolidated version of the profiling algorithm, updated kinetic and photochemical data are taken from the JPL Evaluation n°19-5 (Burkholder et al., 2020). Photolysis rates are computed off-line by using the radiative transfer module of the two-dimensional model SOCRATES (Huang et al., 1998).

The UVSPEC/DISORT RTM is based on the discrete ordinate method and includes a treatment of multiple scattering in a pseudo-spherical geometry approximation. All WF calculations are performed in multiple scattering mode, accounting for the 2D (altitude, SZA) photochemical variation of NO_2 (incident beam only; see Figure 2). The standard altitude grid is 0-90 km with a layer thickness of 2 km. The aerosol extinction profile has been constructed from the aerosol model of Shettle (1989) included in UVSPEC/DISORT. In the stratosphere, the aerosol settings correspond to typical background conditions while in the boundary layer and troposphere, settings representative of a rural environment are used. It should be noted that the UVSPEC/DISORT RTM has been validated through several comparison exercises (Hendrick et al., 2006; Wagner et al., 2007).

In order to retrieve stratospheric NO_2 vertical profiles for globally-distributed stations, LUTs of WFs and 2D (SZA, altitude) fields of NO_2 concentrations are generated for 10° latitude bands between 90°S and 90°N (longitude is fixed to 0°) using the UVSPEC/DISORT-PSCBOX model package initialized with corresponding 3D-CTM meteorological and chemical fields. The other entry parameters are day of the year, altitude of the station, ground albedo, and wavelength (only in the case of the WF LUTs). The a priori profiles needed for the OEM inversion method are extracted from the LUTs of 2D NO_2 concentration fields. Since the standard retrieval altitude range is 0-90km and photochemical model simulations give profile data only from ~10 to ~55 km altitude, the a priori profiles should be complemented below and above this altitude range. Below the lowest model altitude level, a priori profile values are calculated using the following expression: $x_{a,\, level\, i} = 0.5\, x_{a,\, \mathrm{level\, i+1}}$. Thus, the NO_2 tropospheric content in the a priori profile is made negligible for all retrievals. Above the highest model altitude level, the AFGL standard atmosphere (Anderson et al., 1986) completes the NO_2 profile.

Regarding the construction of the a priori covariance matrix S_a, the diagonal values will correspond to a given percentage of the a priori profile and this percentage will be empirically determined for each FRM_4DOAS station based on sensitivity tests. The extra-diagonal terms are added as Gaussian function with a correlation length of 8km.

4 Uncertainty budget assessment

4.1 Systematic uncertainties

In the FRM_4DOAS processing system, the reported systematic uncertainty is the uncertainty of the NO_2 absorption cross sections (used in the spectral fit). The temperature dependence of the NO_2 cross sections should be considered as a quasi-random source of error due to the fluctuations of the stratospheric temperature. It is minimized by applying a temperature correction using a monthly zonal climatology of temperature profiles. An example of application of this temperature correction for the stratospheric NO_2 profile retrieval at the Harestua station is shown in Figure 3.

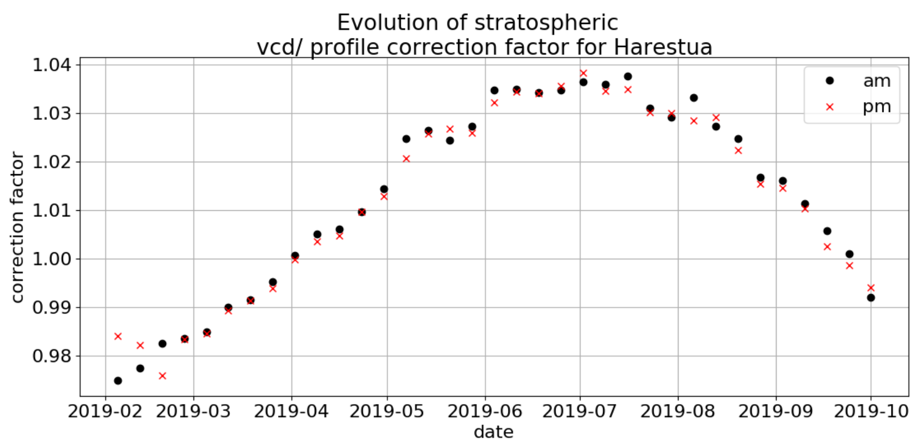

Figure 3: Impact of applying a correction for the temperature dependence of the NO_2 cross sections on the retrieved NO_2 VCDs for one year at the Harestua station. Temperature profiles are extracted from a climatology built up by MPIC based on ECMWF data.

As can be seen, the impact of this correction on the NO_2 VCDs is comprised between -2% in winter and +4% in summer.

4.2 Random uncertainties

In the OEM, the total error of the retrieved profile is the sum of three errors (Rodgers, 2000): the error due to the smoothing of the true profile or smoothing error, the error due to random and systematic errors in the measurements, and the error due to systematic errors in the forward model.

The smoothing error covariance matrix S_s can be calculated using the following expression (Rodgers, 2000):

$S_s = (A - I)\, S_x\, (A - I)^T$ (3)

where S_x is a realistic covariance matrix of the true profile, A is the averaging kernels matrix (see Sect. 5) and I is the identity matrix. S_x also contains extra-diagonal terms in order to account for correlations between trace gas concentration values at different altitude levels. In a first approximation, the S_x matrix is generally chosen identical to S_a.

The retrieval noise S_m which is the retrieval error covariance resulting from measurement error is defined as (Rodgers, 2000):

$$S_m = G\, S_\varepsilon\, G^T \text{ with } G = \frac{\partial \hat{x}}{\partial y} = S_a K^T (K S_a K^T + S_\varepsilon)^{-1} \quad (4)$$

where S_ε is the measurement error covariance matrix, and G is the contribution functions matrix expressing the sensitivity of the retrieved profile to changes in the measured trace gas slant column abundances. As mentioned in Sect. 2, the S_ε matrix was chosen diagonal with values corresponding to the statistical errors on the DOAS fit. For measurement SZAs at which an extra-DSCD error (EDE) should be applied (see Deliverable D-1.1), the statistical error on the DOAS fit is replaced by the EDE when constructing the S_ε matrix. Profile retrievals from twilight zenith-sky measurements at the Bremen station, which is representative of low to moderate pollution conditions, showed that the application of the EDE at some measurement SZAs has a limited impact on the retrieval noise error, as illustrated in Figure 4 below.

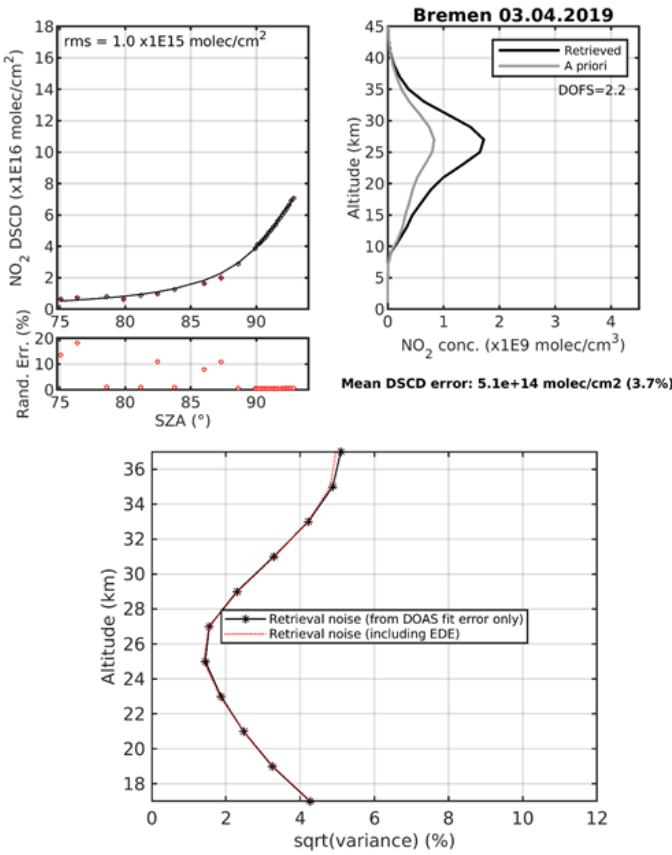

Figure 4: Impact of applying EDE on retrieval noise error. Example (Bremen 03/04/2019 sunrise) of retrieval results obtained when EDE is applied appear on the top row. All the random error values larger than 1% correspond to measurement SZAs where an EDE is applied. The bottom plot shows the retrieval noise error calculated with and without including EDE in the S_ε matrix.

The forward model parameter error S_f is the retrieval error due to errors in the forward model parameters (e.g., errors on the rate constants in the photochemical model). S_f is given by the following expression (Rodgers, 2000):

$$S_f = G\, K_b\, S_b\, K_b^T\, G^T \quad (5)$$

where G is the contribution functions matrix (see Eq. 4), K_b is the sensitivity of the forward model to perturbations of forward model parameters b, and S_b is the covariance matrix of b. S_f cannot be determined easily due to the large number of forward model parameters.

In the current version of the profiling algorithm implemented in the FRM$_4$DOAS processing system, no forward model parameter errors are reported. In the consolidated version, the S_f matrix for stratospheric NO_2 profile will be taken from Preston et al. (1997). This one is derived by calculating the sensitivity of the slant column measurements to large impact forward model (photochemical and/or RT models) parameters like O_3, HNO_3, N_2O_5, aerosol, temperature profiles and ground albedo. To this baseline S_f matrix, forward model parameters errors related to the uncertainty on the NO_2 photolysis rate and the Earth's sphericity correction on the NO_2 WF (see Deliverable D-1.1) will be added in Gaussian quadrature. An example of the different contributions to the total forward model parameters errors is given in Figure 5.

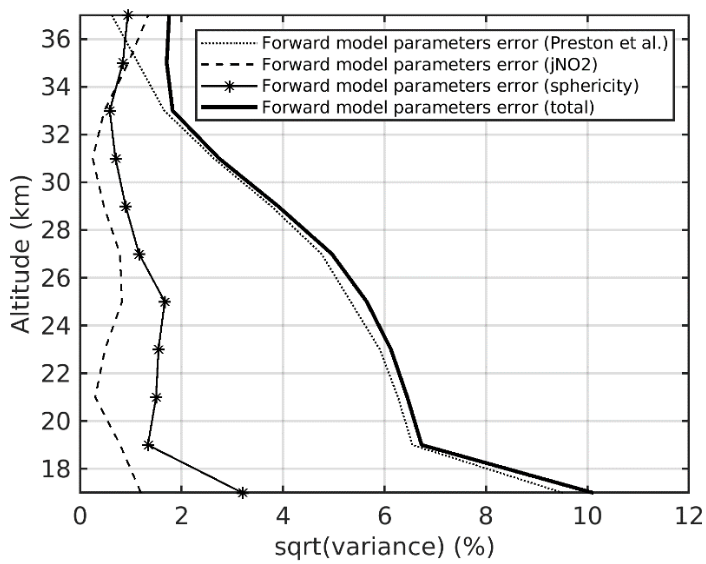

Figure 5: Example (Harestua 10/09/2020 sunset retrieval) of contributions of the different forward model errors that will be implemented in the consolidated profiling algorithm.

In the consolidated profile retrieval, the total forward model parameters will be reported in the level-2 nc output files, as well as the retrieval noise and smoothing errors which are already included in the output files.

5 Vertical resolution/Averaging kernels

The vertical sensitivity of the ground-based zenith-sky twilight measurements to the vertical distribution of trace gases is usually characterized using the AKs (Rodgers, 2000), which correspond to the rows of the averaging kernel matrix A. This matrix is derived using the following expression (Rodgers, 2000):

$$A = \frac{\partial \hat{x}}{\partial x} = (K^T S_\varepsilon^{-1} K + S_a^{-1})^{-1} K^T S_\varepsilon^{-1} K \quad (6)$$

AKs express the relationship between the retrieved profile $\hat{x}$ and the true atmospheric profile x through the following equation:

$$\hat{x} = x_a + A(x - x_a) + \text{Error terms} \qquad (7)$$

Following Eq. (7), the retrieval of any profile point is an average of the entire true profile weighted by the row of the A matrix corresponding to the altitude of the retrieved profile point. For an ideal observing system, the A matrix would be therefore equal to the identity matrix. In the reality, the retrieved profile is only a smoothed perception of the true profile. The vertical resolution of this smoothed information at a given altitude can be estimated by taking the FWHM of the main peak of the corresponding averaging kernel. Another important characterization parameter which can be derived from the A matrix is the number of degrees of freedom for signal (DOFS) providing an estimate of the number of independent pieces of information that can be retrieved from the measurements. This parameter is given by the trace of A (Rodgers, 2000).

Figure 6 shows a typical example of AKs for stratospheric NO_2 OEM-based retrieval.

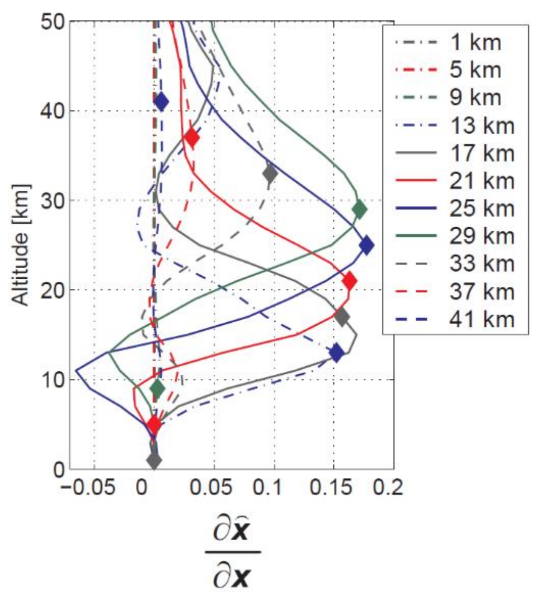

Figure 6: Typical example of AKs for stratospheric NO_2 OEM-based retrieval. Plain diamonds indicate the nominal altitude at which each averaging kernel should peak. (From Hendrick et al., 2004).

From Preston et al. (1997) and Hendrick et al. (2004), it has been found that 13-37 km is the altitude range where twilight zenith-sky measurements give significant information about the vertical distribution of NO_2. From Figure 6, we also see that the vertical resolution is about 8 km at 13 km of altitude and reaches 20 km at an altitude of 33 km. Typical values for the trace of A are about 2-3, meaning that there are about 2-3 independent pieces of information in the measurements.

6 Horizontal representativeness

In contrast to *in-situ* observations such as an NO_2 monitor located at the surface, remote sensing observations provide integrated values representative for values averaged over a certain volume. When evaluating the air volume for which these measurements are representative, a quantity like the horizontal displacement of the measured air volume is usually considered.

For zenith-sky observations, the horizontal displacement of the measurement volume depends mainly on *SZA* and the light path has in first approximation two separate parts: one from the sun to the scattering point in altitude *z* which is determined by the solar position, and a second one passing vertically through the atmosphere from altitude *z* to the instrument on the ground (Figure 7). The horizontal displacement *x* from the instrument location can be computed for each scattering height *z* by:

$$x(z,i) = (i - z).\tan(SZA) \quad (8)$$

For the effective signal, the average over the horizontal displacements for all scattering altitudes *z* needs to be calculated, weighted by the respective radiation received from this altitude at the surface *WF(z)*:

$$d(i) = \frac{\sum_{z,i=0}^{top-atmosphere} x(z,i).WF(z)}{\sum_{z,i=0}^{top-atmosphere} WF(z)} \quad (9)$$

The resulting distances *d,* calculated by using a simple ray-tracing model, are shown in Figure 8 and can be as large as 500 km in the stratosphere at twilight.

In FRM_4DOAS, LUTs of the distance *d* classified according to *SZA* and altitude are used in combination with the solar azimuth angle to report the mean location of the effective air mass corresponding to the retrieved twilight total O_3 columns and stratospheric NO_2 profiles.

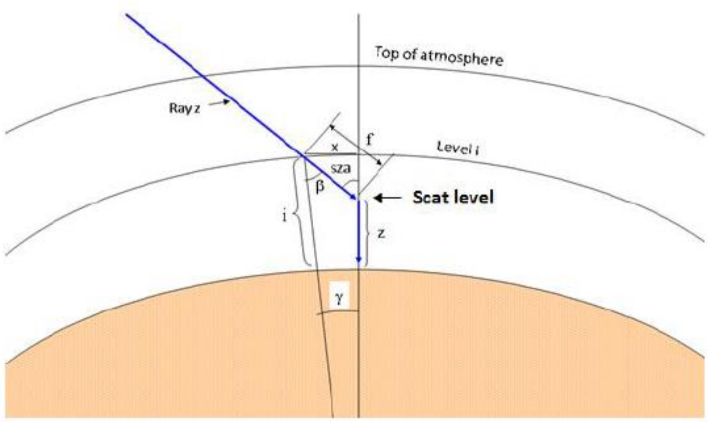

Figure 7: Sketch of the light path for zenith-sky observations. Indicated is the distance *x* that the measurement point has at altitude level *i* for a scattering altitude *z* at solar zenith angle SZA. (From Richter et al., 2013).

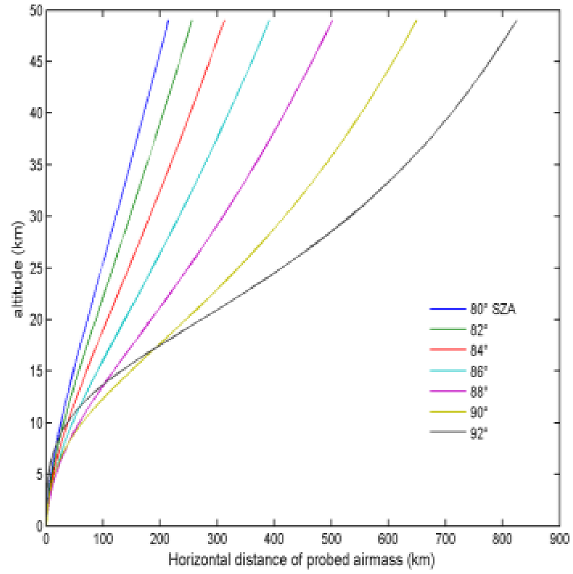

Figure 8: Average displacement of the measurement point in zenith viewing geometry for different altitudes at different solar zenith angles. (From Richter et al., 2013).

7 References

Anderson, G. P., et al., Technical Report: AFGL (Air Force Geophysical Laboratory) atmospheric constituent profiles (0. 120km), Report n° AFGL-TR-86-0110, Air Force Geophysics Lab., Hanscom AFB, MA (USA), 1986.

Barret, B., M. De Mazière, and P. Demoulin, Retrieval and characterisation of ozone profiles from solar infrared spectra at the Jungfraujoch, J. Geophys. Res., 107, doi:10.1029 / 2001JD001298, 2002.

Burkholder, J. B., et al., Chemical Kinetics and Photochemical Data for Use in Atmospheric Studies, Evaluation n°19, NASA JPL Publication n° 19-5, 2020.

Chipperfield, M. P., New version of the TOMCAT/SLIMCAT off-line chemical transport model: Intercomparison of stratospheric tracer experiments, Q. J. R. Meteorol. Soc., 132, 1179-1203, doi:10.1256/qj.05.51, 2006.

Errera, Q., and D. Fonteyn, Four-dimensional variational chemical assimilation of CRISTA stratospheric measurements, J. Geophys. Res., 106 (D11), 12253-12265, 2001.

Hendrick, F., B. Barret, M. Van Roozendael, H. Boesch, A. Butz, M. De Mazière, F. Goutail, C. Hermans, J.-C. Lambert, K. Pfeilsticker, and J.-P. Pommereau, Retrieval of nitrogen dioxide stratospheric profiles from ground-based zenith-sky UV-visible observations: Validation of the technique through correlative comparisons, Atmos. Chem. Phys., 4, 2091-2106, 2004.

Hendrick, F., M. Van Roozendael, A. Kylling, A. Petritoli, A. Rozanov, S. Sanghavi, R. Schofield, C. von Friedeburg, T. Wagner, F. Wittrock, D. Fonteyn, and M. De Mazière, Intercomparison exercise between different radiative transfer models used for the interpretation of ground-based zenith-sky and multi-axis DOAS observations, Atmos. Chem. Phys., 6, 93-108, 2006.

Heskes, H. J. and Boersma, K. F.: Averaging kernels for DOAS total-column satellite retrievals, Atmos. Chem. Phys., 3, 1285–1291, 2003.

Huang, T., S. Walters, G. Brasseur, D. Hauglustaine, W. Wu, S. Chabrillat, X. Tie, C. Granier, A. Smith, S. Madronich, and G. Kockarts, Description of SOCRATES-A Chemical Dynamical RadiativeTwo-Dimensional Model, NCAR Technical Note, NCAR/TN-440+EDD, 1998.

Mayer, B., and A. Kylling, Technical note: The libRadtran software package for radiative transfer calculations - description and examples of use, Atmos. Chem. Phys., 5, 1855-1877, 2005.

Preston, K. E., R. L. Jones, and H. K. Roscoe, Retrieval of NO_2 vertical profiles from ground-based UV-visible measurements: Method and validation, J. Geophys. Res., 102 (D15), 19,089-19,097, 1997.

Richter, A., et al., Spatial Representativeness of NORS observations, Deliverable D4.4 of the EC FP7 NORS project, 2013, https://nors.aeronomie.be/ProjectDir/PDF/D4.4_NORS_SR.pdf

Rodgers, C. D., Inverse Methods for Atmospheric Sounding, Theory and Practice. World Scientific Publishing, Singapore-NewJersey-London-Hong Kong, 2000.

Schofield, R., K. Kreher, B. J. Connor, P. V. Johnston, A. Thomas, D. Shooter, M. P. Chipperfield, C. D. Rodgers, and G. H. Mount, Retrieved tropospheric and stratospheric BrO columns over Lauder, New Zealand, J. Geophys. Res., 109, D14304, doi:10.1029/2003JD004463, 2004.

Shettle, E. P., Models of aerosols, clouds, and precipitation for atmospheric propagation studies, AGARD Conference Proceedings No. 454: Atmospheric propagation in the UV, visible, IR and mm-region and related system aspects, 1989.

Wagner, T., J. P. Burrows, T. Deutschmann, B. Dix, C. von Friedeburg, U. Frieß, F. Hendrick, K.-P. Heue, H. Irie, H. Iwabuchi, Y. Kanaya, J. Keller, C. A. Mc Linden, H. Oetjen, E. Palazzi, A. Petritoli, U. Platt, O. Postylyakov, J. Pukite, A. Richter, M. Van Roozendael, A. Rozanov, R. Sinreich, S. Sanghavi, S., and Wittrock, F. : Comparison of box-air-mass-factors and radiances for multiple-axis differential optical absorption spectroscopy (MAX-DOAS) geometries calculated from different UV/visible radiative transfer models, Atmos. Chem. Phys., 7, 1809-1833, 2007.